

Data Acquisition via Experimental Design for Decentralized Data Markets

Charles Lu
Massachusetts Institute of Technology

Baihe Huang
University of California, Berkeley

Sai Praneeth Karimireddy
University of California, Berkeley

Praneeth Vepakomma
Massachusetts Institute of Technology

Michael I. Jordan
University of California, Berkeley

Ramesh Raskar
Massachusetts Institute of Technology

Abstract

Acquiring high-quality training data is essential for current machine learning models. Data markets provide a way to increase the supply of data, particularly in data-scarce domains such as healthcare, by incentivizing potential data sellers to join the market. A major challenge for a data buyer in such a market is selecting the most valuable data points from a data seller. Unlike prior work in data valuation, which assumes centralized data access, we propose a federated approach to the data selection problem that is inspired by linear experimental design. Our proposed data selection method achieves lower prediction error without requiring labeled validation data and can be optimized in a fast and federated procedure. The key insight of our work is that a method that directly estimates the benefit of acquiring data for test set prediction is particularly compatible with a decentralized market setting.

1 Introduction

Recent breakthroughs in machine learning have heavily depended on the general availability and access to massive amounts of training data. Such collections are still, however, mostly the province of large companies, and it is an important agenda item for machine learning researchers to develop mechanisms that allow greater data access among smaller players. A related point is that many data providers have become resistant to having their data simply collected without their consent or without their participation in the fruits of predictive modeling. These trends motivate the study of *data marketplaces*, which aim to incentivize data sharing between buyers and sellers Castro Fernandez (2023); Agarwal et al. (2019); Travizano et al. (2020).

In many applications, a data buyer has a specific goal in mind, and in particular wants to acquire training data to predict their test data in a specific context. For example, the buyer may be a patient who cares about diagnosing their own chest X-ray and is willing to pay some fixed budget to access other X-rays to train a model to have low error on their “test set.” The revenue generated from the

buyer’s payment should be allocated according to how useful a seller’s data point was in answering the buyer’s query.

In this paper, we argue that current data valuation techniques are insufficient for the data market setting. We propose a fast, federated data selection method based on experimental design that achieves lower prediction error compared to centralized baselines. Unlike previous data valuation approaches, our method does not require a labeled held-out validation set and instead directly optimizes data selection for the buyer’s unlabeled test data. This direct approach to data valuation avoids the issue of “inference after selection,” which can lead to overfitting on the validation set (Vapnik, 1999; Bartlett et al., 2002). Additionally, our approach naturally solves the problems of budget allocation and revenue simultaneously, which is rarely addressed together in current work in data valuation Zhao et al. (2023).

In summary, our contributions are the following:

1. Analyze the challenges of current data valuation approaches for decentralized data markets,
2. Propose a novel data acquisition procedure based on experimental linear design (see Figure 1),
3. Design a scalable iterative algorithm using the Frank-Wolfe method (1956) to solve the objective.
4. Demonstrate state-of-the-art performance on several real-world medical datasets.

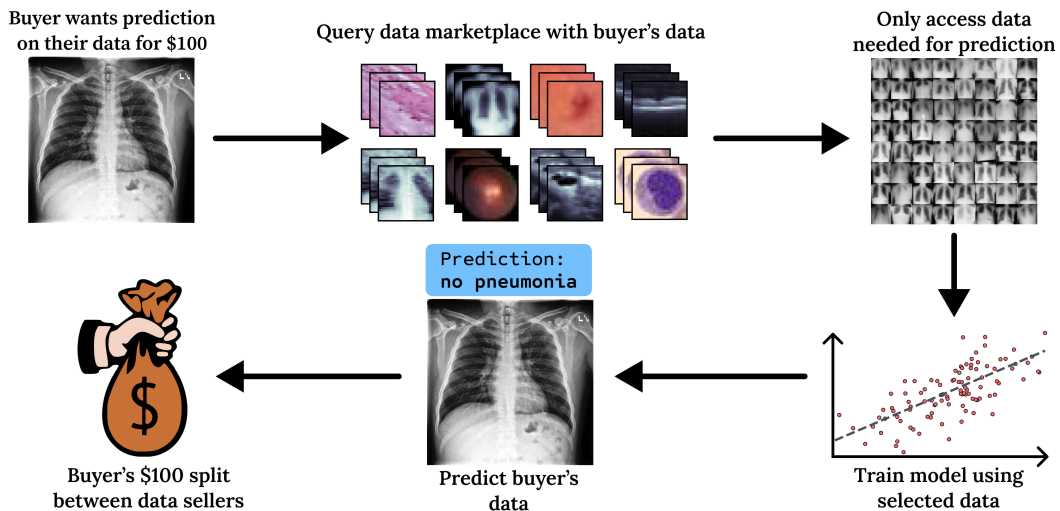


Figure 1: **Overview of data acquisition process between buyer and seller.** In contrast with other data selection approaches, our method uses the buyer’s unlabeled data to select a subset of seller data points. The selected data is then used to train a regression model to predict the buyer’s test data. Our data selection method is optimized in a federated and scalable manner.

2 Challenges with Current Data Valuation Approaches

The topic of “data valuation” is exemplified by the Data Shapley value approach Ghorbani & Zou (2019), which measures the marginal contribution of each training data point’s influence on a specified

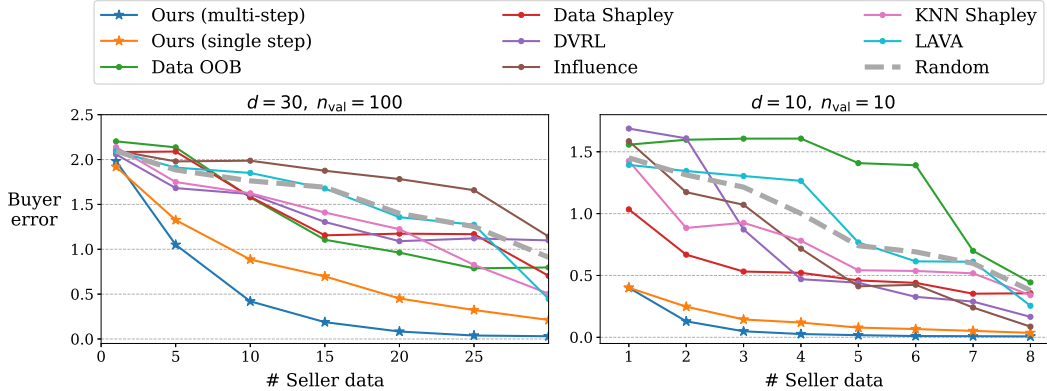


Figure 2: **Current data valuation methods overfit data is high-dimensional or with the validation set is small.** In the left subplot, we see that data valuation methods overfit when the dimensionality is high. For instance, with IID Gaussian data in 30 dimensions, common data attribution methods such as KNN Shapley overfit the validation set, with several data valuation methods performing similarly to the random selection baseline. In the right subplot, we see that data valuation methods can also overfit when the number of samples in the validation set is small. In contrast, our method does not use a validation set and optimizes the unlabeled test data directly. Both training and testing data are drawn IID from a Gaussian distribution, and results are averaged over 100 different buyer test points.

utility function, usually evaluated as an improvement on a validation set. We distinguish between *attributing* the influence of training data on validation performance and *valuing* data for its usefulness in predicting unseen test data. We contend that current data valuation methods, such as Data Shapley and its variants, that measure the change in the model’s validation performance should not be conflated with the data value for training a model to achieve low test error. While these data attribution methods can help gather insight into model behavior on a particular data point,¹ data validation techniques that rely on a validation set can overfit, even on IID data.

In Figure 2, we illustrate this issue by showing how current data valuation methods overfit when the data dimension is large and when the validation set is small. For a simple experiment, the data seller has 1,000 available training data points, and the buyer has a single test data point, all sampled IID from a Gaussian distribution. The goal is to select a subset of seller data points to train a regression model to attain low prediction error on the buyer’s data.

In both experiments, we see that other data valuation techniques have poor test prediction errors—some techniques even underperform the baseline of randomly selecting seller data. Our proposed method maintains low test error as more seller training data is selected. This experiment demonstrates that attributing the influence of training data to validation performance is not the same as estimating data value for making test-time predictions on new data. To support this argument, we provide a theoretical analysis to bound test error in Section 3.2.

Another difference between our approach and previous work is the assumption of centralized data access to perform the valuation. In a decentralized data marketplace, data validation must be

¹Indeed, Shapley-based techniques were previously introduced to quantify feature importance to aid in model interpretability Štrumbelj & Kononenko (2014), such as the popular SHapley Additive exPlanations (SHAP) framework Lundberg & Lee (2017). Data Shapley Ghorbani & Zou (2019) repurposes Shapley values to explain the marginal contribution of a data point (rows of the design matrix) rather than the features (columns of the design matrix), hence the name *Data Shapley* to differentiate from Feature Shapley.

performed before full data access is granted to the buyer Kennedy et al. (2022). This is related to Arrow’s Information Paradox Arrow (1972), where a seller would be unwilling to give access before payment because data can be easily copied. At the same time, a buyer would be unlikely to purchase data without first determining its value, quality, relevance, etc. This distinction between centralized and decentralized techniques for data markets is becoming widely appreciated. A recent data valuation benchmark motivates the need to estimate value without requiring white-box access to the seller’s data Chen et al. (2023).

3 Methods

3.1 Market Description

In our model of a data market, the interaction between the buyer and the data seller unfolds as follows:

1. The buyer brings their test data $(X^{\text{test}}, Y^{\text{test}})$, where $X^{\text{test}} = (x_1^{\text{test}}, \dots, x_m^{\text{test}})$ and $Y^{\text{test}} = (y_1^{\text{test}}, \dots, y_m^{\text{test}})$, with the aim of obtaining the best possible predictions over the test data within budget B .
2. There are a total of n sellers in the market where each seller i possesses a data point (x_i, y_i) with a marginal price c_i specified for their data.
3. Given *only the covariates* $X^{\text{test}} = (x_1^{\text{test}}, \dots, x_m^{\text{test}})$, the platform determines a weight w_i to assign to each data point (x_i, y_i) . This weight, w_i , can represent (1) the sampling probability of data point i , (2) the “usage” of data point i in training the model f_θ , (3) or the privacy budget (e.g., the ϵ parameter in the differential privacy framework of Dwork et al. (2006)) associated with that particular data point in the algorithm.
4. The platform selects the data points from the sellers according to the weights (w_1, \dots, w_n) and trains a model $f_{\hat{\theta}(w)}$ using this data. The trained model is given to the buyer, and each seller receives compensation equal to $c_i \cdot w_i$ for their respective data point.

Under this framework, the problem for the platform is to pick the $w = (w_1, \dots, w_n)$, which minimizes the expected prediction error for the buyer while adhering to their budget constraint $\sum_{j=1}^n w_j c_j \leq B$. This gives rise to the following problem:

$$\begin{aligned} \max_{w \in \mathbb{R}_+^n} \mathcal{L}(w) &:= \frac{1}{m} \sum_{i \in [m]} \mathbb{E}_{y_i^{\text{test}}} \left[l \left(f_{\hat{\theta}(w)}(x_i^{\text{test}}), y_i^{\text{test}} \right) \right] \\ \text{s.t.} \quad &\sum_{j=1}^n w_j c_j \leq B. \end{aligned} \tag{1}$$

Note that this problem can not be solved directly because the target $(y_i^{\text{test}})_{i=1}^m$ is not accessible to the platform. To address this problem, we model the targets Y^{test} and $Y^{\text{train}} = (y_1, \dots, y_n)$ as following the same (conditional) distribution $\mathcal{D}_{y|x}: y = f_{\theta_*}(x) + e$, where f is a parametric model, θ_* is the underlying parameter, and e is the error term from a distribution \mathcal{E} such that $\text{Var}(e) = \sigma^2$. Furthermore, we let \mathcal{D}_X denote the test distribution of the covariates x_i^{test} . Note that we do not impose any assumption on $X^{\text{train}} = (x_1, \dots, x_n)$ allowing it to arise from a distribution other than \mathcal{D}_X . We contrast two approaches to solving this problem in the next two subsections.

3.2 Folly of relying on validation data

In data Shapley value (Ghorbani & Zou, 2019), the model’s performance is evaluated using a validation set $\{(x_j^{\text{val}}, y_j^{\text{val}}), j = 1, \dots, n_{\text{val}}\}$, where the x_j^{val} are sampled from the test distribution \mathcal{D}_X and the y_j^{val} follow the same conditional distribution $\mathcal{D}_{Y|X}$. This gives rise to the first approximation of Problem (1):

$$\begin{aligned} \max_{w \in \mathbb{R}_+^n} \quad & \sum_{j=1}^{n_{\text{val}}} l\left(f_{\hat{\theta}(w)}(x_j^{\text{val}}), y_j^{\text{val}}\right) \\ \text{s.t.} \quad & \sum_{j=1}^n w_j c_j \leq B. \end{aligned} \quad (2)$$

However, this approach heavily relies on the quantity and quality of the validation dataset. In fact, we have the following minimax lower bound.

Theorem 1. *Let w^* denote the solution of Problem (1) and let \hat{w} denote the solution of Problem (2). Suppose \mathcal{D}_X is supported on B_R^d (zero-centered ball with radius R in \mathbb{R}^d) and l is square loss, then there exist numerical constants, c_1, c_2, c_3 , such that:*

(i) *With probability at least $1 - \exp(-c_1 n_{\text{val}}/R^2)$,*

$$\inf_{\hat{\theta}} \sup_{\mathcal{D}_{Y|X}, X^{\text{train}}} \mathbb{E}_{X^{\text{test}}} [\mathcal{L}(\hat{w}) - \mathcal{L}(w^*)] \geq \frac{c_2 \sigma^2 d}{n_{\text{val}}}.$$

(ii) *If there exists $\kappa > 0$ such that $\lambda(\mathbb{E}_{x \sim \mathcal{D}_X}[x^{\otimes 4}]) \leq \kappa \cdot \lambda(\mathbb{E}_{x \sim \mathcal{D}_X}[x^{\otimes 2}]^{\otimes 2})$, then for any training algorithm used by the platform, with probability at least $0.99 - \exp(-c_1 n_{\text{val}}/R^2) - \frac{c_3 \kappa}{\kappa + m}$, we have*

$$\sup_{\mathcal{D}_{Y|X}, X^{\text{train}}} \mathcal{L}(\hat{w}) - \mathcal{L}(w^*) \geq \frac{c_2 \sigma^2 d}{n_{\text{val}}}.$$

This result implies that for the validation-based approach, its expected test error scales as at least d/n_{val} in the worst case, with high probability, and with constant probability, its error on buyer’s data scales as at least d/n_{val} . The dependence on the dimension d and the number of validation points n_{val} highlights that this method may be suboptimal in high-dimensional settings or when the validation dataset is small. Furthermore, it is challenging for the buyer (or the platform) to acquire ground-truth labels in many real-world applications. We conclude that such approaches, which includes the Data Shapley value approach of Ghorbani & Zou (2019), are not well-suited for data markets.

3.3 Linear experimental design

Optimal experiment design deals with selecting the training data that maximizes the information matrix \mathcal{I} under certain criterion. Consider the similar setting in Theorem 1 where l is square loss and there is a feature function $\phi : \mathcal{X} \rightarrow \mathbb{R}^{d_0}$ that $y = \theta^\top \phi(x) + \sigma \cdot \epsilon$ (ϵ is standard Gaussian noise), then the test loss of the Least Square (LS) estimator trained on X_{train} , denoted by $\hat{\theta}_{X_{\text{train}}}$, has the

following explicit quantification:

$$\begin{aligned} & \frac{1}{m} \sum_{i=1}^m \mathbb{E} \left[l \left(f_{\hat{\theta}(w)}(x_i^{\text{test}}), y_i^{\text{test}} \right) \mid X_{\text{train}}, X_{\text{test}} \right] \\ &= \frac{1}{m} \sum_{i=1}^m \phi(x_i^{\text{test}})^\top \left(\sum_{j=1}^n w_j \phi(x_j) \phi(x_j)^\top \right)^{-1} \phi(x_i^{\text{test}}). \end{aligned}$$

Therefore, we arrive at the following optimization problem

$$\begin{aligned} & \max_{w \in \mathbb{R}_+^n} \sum_{i=1}^m (z_i^{\text{test}})^\top \left(\sum_{j=1}^n w_j z_j z_j^\top \right)^{-1} (z_i^{\text{test}}) \\ & \text{s.t.} \quad \sum_{j=1}^n w_j c_j \leq B. \end{aligned} \tag{3}$$

where $z_j = \phi(x_j)$, $z_i^{\text{test}} = \phi(x_i^{\text{test}})$. We advocate this method for the following reasons. First, it does not require ground-truth labels in the test dataset X^{test} to be provided by the buyer, thereby improving the flexibility of the type of allowable marketplace settings. Instead, this formulation only uses unlabeled data points, which are often abundant. Second, applying linear optimal design, Eq. (3) gives the exact optimal solution in linear regression. Third, in many ML applications, the model is locally linear where the trainable parameters only move a short distance from initialization (e.g., in the “lazy” regime of wide neural networks (Du et al., 2019; Jacot et al., 2018; Allen-Zhu et al., 2019) and in fine-tuning of large language/vision models (Kornblith et al., 2019; Hu et al., 2021; Wei et al., 2021)). In this context, the loss function can be further approximated by a quadratic function endowed with the local curvature. Therefore, our experiment design method can be widely applied to deal with general data market problems.

3.4 Fast and federated optimization

If we constrain w to be the probability simplex Δ^m , then our cost objective is the following:²

$$\arg \min_{w \in \Delta^n} \left\{ C(w) := \mathbb{E}_{x_0 \sim \mathcal{D}} \left[x_0^\top P(w) x_0 \right] \right\}, \tag{4}$$

where $P \in \mathbb{R}^{d \times d}$ is the inverse information matrix, defined as

$$P(w) := \left(\sum_{j=1}^n w_j x_j x_j^\top \right)^{-1}. \tag{5}$$

Then, the gradient of the cost function simplifies to:

$$\nabla_{w_j} C(w) = - \left(\mathbb{E}_{x_0 \sim \mathcal{D}} \left[x_0^\top P(w) x_j \right] \right)^2. \tag{6}$$

Given the value of $P(w)$, the above gradient is relatively easy to compute. In fact, it can be computed *using only local seller data* x_j . Hence, the gradient computation is trivially federated, with each seller computing only the coordinates corresponding to their data points x_j .

Our optimization strategy uses the Frank-Wolfe algorithm (Frank et al., 1956; Jaggi, 2013) to update the w vector iteratively. We *shrink all weights* by $(1 - \alpha)$ and increase the weight of the

²We overload $x_j := \phi(x_j)$ and $x_0 := \phi(x_0)$ for the rest of this section.

Algorithm 1 Optimization Procedure

```

1: Input: Buyer test point  $x_0 \in \mathbb{R}^d$ , Seller data points  $X \in \mathbb{R}^{n \times d}$ , Seller weights  $w \in \mathbb{R}^n$ , iteration
   steps  $T$ , and  $K$  number of points to select
2: Output: Subset of seller data points  $X' \in \mathbb{R}^{n' \times d}$ , where  $n' < n$ 
3:  $w \leftarrow \mathbb{1}/n$  # Initialize weight vector
4:  $P_0 \leftarrow (X^\top \text{diag}(w)X)^{-1}$  # Can also initialize  $P$  to  $\mathbb{I}$ 
5: for  $t = 1 \dots T$  do
6:    $C \leftarrow \mathbb{E}_{x_0} [x_0^\top P x_0]$  # Compute design loss
7:    $g \leftarrow -\nabla C(w)$  # Compute negative gradients
8:    $j_t \leftarrow \arg \max_j g_j$  # Select largest coordinate
9:    $\alpha \leftarrow \text{LINE\_SEARCH}(C)$  # (Optional) Find step size
10:   $w \leftarrow (1 - \alpha)w, P \leftarrow 1/(1-\alpha)P$  # Shrink weights
11:   $w_{j_t} \leftarrow w_{j_t} + \alpha$  # Increase weight
12:   $u \leftarrow \sqrt{\alpha}X[j_t]$  # Update chosen data point
13:   $P \leftarrow \text{SHERMAN\_MORRISON}(P, u, u^\top)$ 
14: end for
15:  $X' \leftarrow X[\text{TOP\_K}(w, K)]$  # Select data points using  $w$ 

```

coordinate with the largest negative gradient.

$$w \leftarrow (1 - \alpha)w + \alpha e_{j_t}$$

$$j_t := \arg \max_j -\nabla_{w_j} C(w)$$

Computing the max gradient coordinate requires communication among the sellers, but is very communication-efficient to implement — they only send a single scalar.

Further, note that with Frank-Wolfe, the update to the information matrix will be *rank 1* at each iteration. Hence, we can efficiently update the $P(w)$ matrix using the Sherman–Morrison formula (Sherman & Morrison, 1950):

$$P \leftarrow \frac{1}{1 - \alpha} P - \frac{\alpha P x_{j_t} x_{j_t}^\top P}{1 + \alpha x_{j_t}^\top P x_{j_t}}. \quad (7)$$

This update only involves the current P matrix and the single data point x_j selected for the round, which can be locally computed by the seller. Further, the seller can also locally evaluate the updated cost $C(w)$ as in eqn. (4) for any α :

$$C(w) = \frac{1}{1 - \alpha} \mathbb{E}_{x_0} [x_0^\top P x_0] - \frac{\alpha}{1 + \alpha x_{j_t}^\top P x_{j_t}} \mathbb{E}_{x_0} (x_0^\top P x_{j_t})^2$$

Thus, they can optionally perform a line search to find the best step size α (or even compute it in closed form). After, the seller can communicate the α and x_{j_t} to the rest of the sellers to compute the updated P using only $O(d)$ communication. Our complete optimization procedure is summarized in Algorithm 3.4.

We can also forgo the iterative process and only use a single iteration. This is equivalent to replacing our cost function with a linear approximation and selecting the top k seller data points using

$$\mathcal{W}(k) = \text{Top-K} \left(\left\{ \mathbb{E}_{x_0 \sim \mathcal{D}} [x_0^\top P(\frac{1}{n}) x_j]^2 \right\}_{x_j \in \mathcal{X}_{\text{train}}} \right)$$

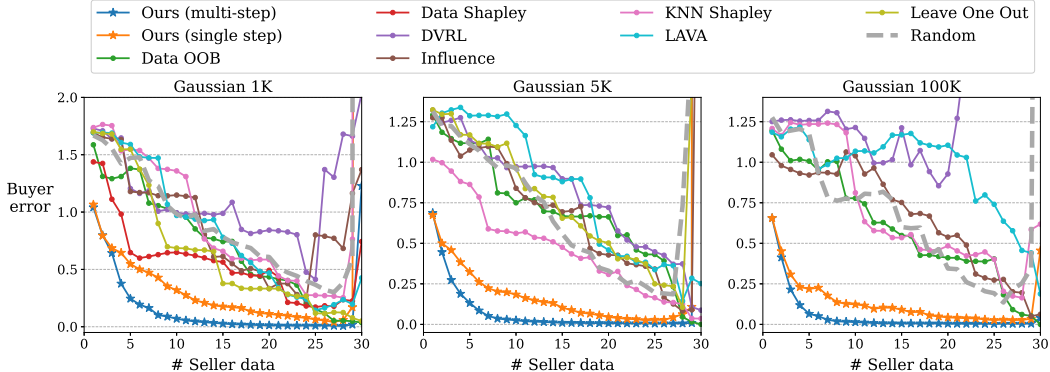


Figure 3: **Comparing data valuation methods on Gaussian distributed data when the seller has 1K, 5K, and 100K data points.** After optimization, each data valuation method selects the top- k most valuable data points from the seller to train a regression model to predict the buyer’s test data. Our data selection algorithm based on experimental design achieves better test MSE on the buyer’s data with fewer training points. Results are plotted as the average over 100 different buyers.

We term this variant **single step**. As we will see experimentally, this simplified version of the algorithm is extremely fast while maintaining relatively good performance.

In Appendix D.4, we compare the federated optimization procedure with a convex optimization solver (CVXPY, Diamond & Boyd, 2016) and find that the iterative approach results in several orders of magnitude speedup while maintaining similar test performance.

3.5 Regularization

We $d > n$ or when d is large, the initial computation of the inverse information matrix may be ill-conditioned and may benefit from shrinkage regularization $\lambda \in [0, 1]$:

$$P_{\text{Reg}} = ((1 - \lambda) \cdot (X^\top \text{diag}(w) X) + \lambda \cdot \sigma_X^2 \mathbb{I})^{-1}, \quad (8)$$

where \mathbb{I} is the identity matrix, diag is the diagonal operator, and σ_X^2 is the variance of the features of X .

When $\lambda = 1$, the initialization of P does not depend on the seller data X , and the optimization procedure can be more fully decentralized; otherwise, one can employ private estimation of the initial information matrix (Dwork, 2006).

4 Experiments

We evaluate our data selection algorithm on several real-world medical datasets in several practical configurations, such as when x is embedded through deep representations, when $\{x_j\}_{j=1}^m$ has heterogeneous costs $\{c_j\}_{j=1}^m$, and when the buyer data x_0 consists of multiple test data points $\{x_i\}_{i=1}^m$. We compare scalability between selection algorithms and also perform several ablation experiments to evaluate the choice of optimization steps and the amount of regularization on the initialization of the information matrix.

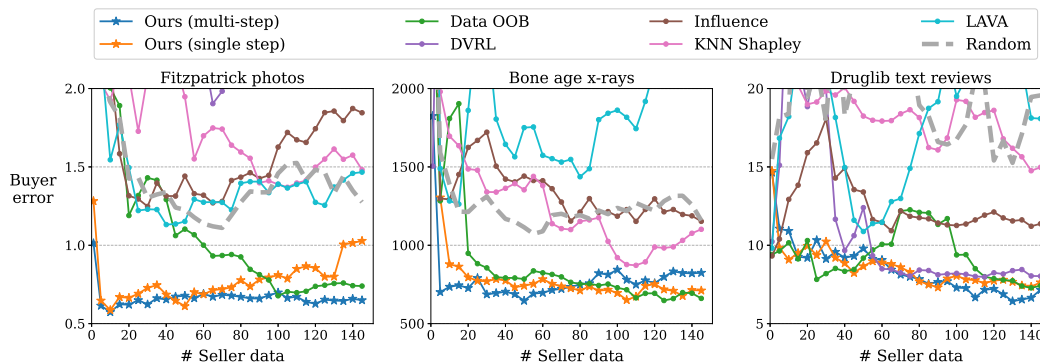


Figure 4: **Our method works on data embedding through CLIP and GPT-2.** We compare our method against other data valuation methods on two medical imaging datasets (Fitzpatrick17K and RSNA Bone Age) embedded through CLIP and the DrugLib review dataset embedded through GPT-2. After optimization, each data valuation method selects the top- k most valuable data points from the seller to train a regression model to predict the buyer’s test data. Our data selection algorithm based on experimental design achieves lower prediction mean squared error on the buyer’s data with fewer training points. Results are plotted as the average over 100 different buyers.

4.1 Datasets and setup

In addition to synthetic Gaussian data (see Appendix C for code implementation), we also use the following medical datasets for evaluation:

1. **Fitzpatrick17K** Groh et al. (2021) skin lesion dataset, where the task is to predict Fitzpatrick skin tone, an ordinal 6-point scale in 0.5 intervals, from dermatology images.
2. **RSNA Pediatric Bone Age dataset** Halabi et al. (2019) where the prediction task is to assess bone age (in months) from hand X-ray images.
3. **Medical Information Mart for Intensive Care (MIMIC-III)** Johnson et al. (2016), where the task is to predict the length of hospital stay from 46 clinical attributes.
4. **DrugLib reviews** Kallumadi & Grer (2018), text reviews of drugs where the task is to predict subject ratings (1-10).

For the Bone Age X-ray and Fitzpatrick skin type datasets, we embed the data through a CLIP model (ViT-B/32) Radford et al. (2021), resulting in a 512-dimensional vector for each image. For the DrugLib drug review dataset, we embed each text review through a GPT-2 Radford et al. (2019) model with a max context length of 4096, resulting in a 784-dimensional vector for each review (see Appendix C for the prompt template). For each data selection method, we optimize a single buyer point using a validation set of 100 samples and average results over 100 random buyers. For more details on experimental setup, see Appendix C.

4.2 Main results

Performance versus data valuation methods. In Figure 3, we compare our method against other data valuation methods on the synthetic Gaussian dataset with varying amounts of available seller

Method	Gaussian		MIMIC		Bone age	Fitz.	Druglib
	1K	100K	1K	35K	12K	15K	3.5K
Random baseline	1.38	1.01	301.0	283.7	1309.1	1.49	21.4
Data Shapley Ghorbani & Zou (2019)	0.87	N/A	294.9	N/A	N/A	N/A	N/A
Leave One Out Cook (1977)	1.31	N/A	1125.0	N/A	N/A	N/A	N/A
Influence Feldman & Zhang (2020)	1.47	0.97	189.4	876.4	1614.5	1.93	12.8
DVRL Yoon et al. (2020)	1.33	1.26	229.7	285.5	3528.8	3.00	12.6
LAVA Just et al. (2023)	1.47	1.10	190.9	417.3	1867.5	1.45	17.4
KNN Shapley Jia et al. (2019)	1.55	1.18	175.7	229.6	1387.0	1.82	19.0
Data OOB Kwon & Zou (2023)	1.24	0.98	169.7	<u>215.6</u>	1020.3	1.35	10.0
Ours (single step)	<u>0.58</u>	<u>0.27</u>	277.4	659.9	900.2	<u>0.73</u>	9.0
Ours (multi-step)	0.37	0.16	<u>206.7</u>	171.4	785.2	0.67	<u>9.2</u>

Table 1: **Our method achieves a lower buyer error than other common data valuation methods.** We compared the test mean squared error on the buyer test point on a synthetic Gaussian dataset and four medical datasets: Mimic, Bone Age, Fitzpatrick, and Druglib. The subheading denotes the number of seller training data available for that experiment, and “N/A” denotes that the method exceeded runtime constraints for the experiment. We optimize a separate random sample of training and validation data for each buyer and average over 100 buyers. Bolded values indicate the best-performing method and underlined values denotes the second-best-performing method.

data. Our method has the lowest test mean squared error (MSE), and this gap increases with the amount of data available for selection.

In Figure 4, we plot error curves for three real-world datasets: two medical imaging (Fitzpatrick skin type and RSNA Bone Age X-ray) that were embedded through CLIP and the DrugLib reviews dataset that was embedded through GPT-2. We see that both multi-step and single-step variants of our method perform well against other data valuation methods, highlighting that our method works on embeddings of high-dimensional data.

Table 1 summarizes our results on all datasets. For the Gaussian and MIMIC datasets, we report the mean error of selecting $\{1, 2, 3, \dots, 10\}$ seller points, while for the embedded datasets (Bone age, Fitzpatrick, Druglib), we report the mean error of selecting $\{1, 5, 10, \dots, 100\}$ seller points for each method.

Data selection with heterogeneous costs. We next consider the setting where the seller data have non-homogeneous costs across the data points. We uniformly sample costs $c \in \{1, 2, 3, 4, 5\}$ for each seller point and add cost-dependent label noise $\tilde{\epsilon} := \bar{y}\epsilon$, $\epsilon \sim \mathcal{N}$, to each data point $\tilde{y}_i := y_i + \beta\tilde{\epsilon}/h(c_i)$, where \bar{y} is the mean target, h is some cost function, and β is the noise level, which we fix to 30% throughout our experiments. We divide the gradient (Equation 6) of each data point by the cost associated with that data point ∇_{w_i}/c_i .

In Figure 5, we show the results on the Bone Age dataset for the squared cost function $h(c) = c^2$. We observe that our multi-step method achieves lower error for a range of budget constraints under this label noise setting compared to other data selection methods. We report additional budget experiments on other datasets and for different cost functions in Appendix D.2 and summarize results in Table 2.

Comparing optimization runtime. In Figure 6, we compare the optimization runtime of each data selection method on 1,000 data points from a 30-dimensional Gaussian distribution. Our single-step method had the fastest runtime, while our multi-step method with 500 steps is competitive against efficiency-optimized valuation techniques such as KNN Shapley Jia et al. (2019). We also compare runtime as we increase the dimensionality of the data (in Fig. 15) and as the amount of seller

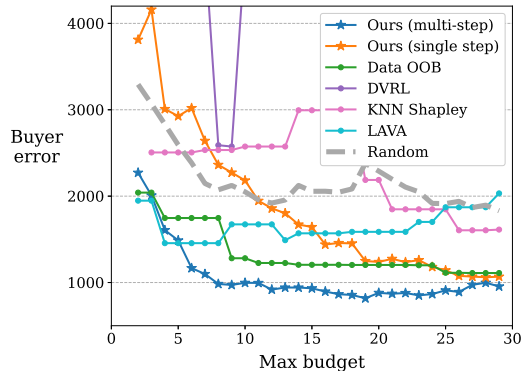


Figure 5: **Comparing error under budget constraints on Bone Age X-ray dataset.** Costs are sampled from $c \in \{1, 2, 3, 4, 5\}$ with a squared cost function $h(c) = c^2$. Chosen from seller 12,000 points and averaged over 100 buyer test points.

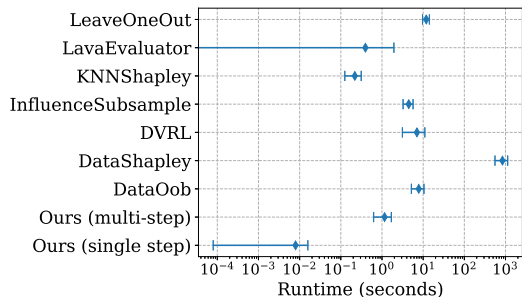


Figure 6: **Our method has a fast optimization runtime compared with other data selection methods.** We compare data selection time on 1,000 Gaussian data points in 10 dimensions and average over 100 separate optimization runs.

data is increased (in Figure 14). We find that our method is highly scalable in both the number of dimensions and the number of data points.

4.3 Ablation Experiments

Amount of buyer data. In Figure 7, we evaluate our method’s performance when the buyer has multiple test points. While in our experimental setup, all buyer and seller data is sampled IID from the same dataset, the amount of buyer data will still affect the optimization procedure. In Figure 7, we vary the number of data points in the “test batch” while fixing 10,000 seller data points from a 30-dimensional Gaussian distribution. We find that beyond a test batch of 5–10 points, the test error generally increases across the amount of selected seller data. Additional datasets are provided in Appendix D.6.

Strength of regularization. In Figure 8, we vary the amount of regularization applied to the information matrix at initialization using the MIMIC-35K dataset. We find that applying a moderate amount of regularization λ between (0.2, 0.6) can lead to improved performance. Even when no real data is used to compute the information matrix, i.e. $\lambda = 1$, the performance is still quite

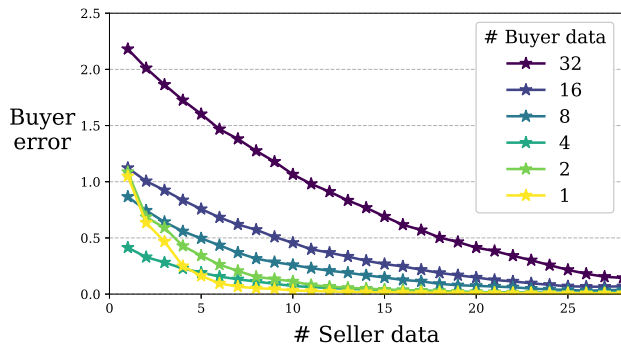


Figure 7: **Varying number of test points optimized.** We plot buyer error by optimizing for an increasing number of test points on 10,000 seller data points from a 30-dimensional Gaussian dataset. We find that increasing the number of buyer points to simultaneously optimize also increases test error.

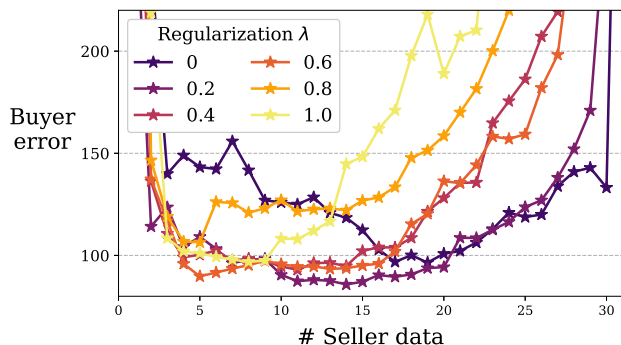


Figure 8: **Effect of regularization strength.** We vary the amount of regularization on the initial information matrix on the MIMIC-35K dataset. We find that applying a moderate amount of regularization improves performance.

reasonable—implying that our data selection procedure may not require the real information matrix to be computed. Results on other datasets are included in Appendix D.5.

Number of optimization steps. In Appendix D.7, we vary the number of optimization steps in our data selection method on the Gaussian and Bone Age datasets. We find that more iterations of optimization generally lead to improved prediction performance, especially when selecting more seller data. Intuitively, one expects that selecting K points requires at least K steps of iterative optimization, which seems to agree with our experiments.

5 Discussion

Our data selection method based on experimental design outperformed all other data valuation methods under several experimental settings. Notably, our single-step variant still maintained good performance on most datasets and outperformed all competing methods in terms of total runtime.

When the seller’s data have heterogeneous costs across data points, our method is more budget-efficient as well.

As discussed in Section 2 and Section 3.2, the existing paradigm of valuing data with a validation set is suboptimal. Incidentally, the second-best performing method, Data OOB Kwon & Zou (2023), is the only other method we compared against that does not use a validation set.

Moreover, a major advantage of our method is that it is amendable to federated optimization requiring $O(d)$ communication per round, making it well-suited for decentralized data markets, unlike other methods that require seller data to be centralized in order to repeatedly train models to estimate data value. Because data is easily duplicated, a seller would not allow access before payment. Additionally, our method does not require labeled data, whereas all other data valuation methods assume that all data come with corresponding ground-truth labels.

However, our algorithm comes with some limitations that form exciting directions for future work. It currently communicates every step. Instead, integrating local steps like in FedAvg McMahan et al. (2017) or SCAFFOLD Karimireddy et al. (2020) would decrease communication costs. Further, integrating differential privacy techniques would provide formal privacy guarantees to the buyers and sellers.

6 Conclusions

In many practical scenarios involving data markets, a buyer may not want to acquire all available data for sale but only a subset of data that is most relevant to their prediction problem. In this paper, we focus on the data selection problem for a buyer who wants to acquire training data to predict their test data. Informed by theoretical insights from optimal experimental design, our method directly optimizes data selection using the buyer’s data. We find that compared to current data selection methods that rely on a validation set to measure data value, our approach achieves lower prediction error and is computationally efficient, making it well-suited for decentralized data market settings.

References

- Agarwal, A., Dahleh, M., and Sarkar, T. A marketplace for data: An algorithmic solution. In *Proceedings of the 2019 ACM Conference on Economics and Computation*, pp. 701–726, 2019.
- Allen-Zhu, Z., Li, Y., and Song, Z. A convergence theory for deep learning via over-parameterization. In *International conference on machine learning*, pp. 242–252. PMLR, 2019.
- Arrow, K. J. *Economic welfare and the allocation of resources for invention*. Springer, 1972.
- Bach, F., Lacoste-Julien, S., and Obozinski, G. On the equivalence between herding and conditional gradient algorithms. In *International Conference on Machine Learning*, 2012.
- Bartlett, P. L., Boucheron, S., and Lugosi, G. Model selection and error estimation. *Machine Learning*, 48:85–113, 2002.
- Castro Fernandez, R. Data-sharing markets: Model, protocol, and algorithms to incentivize the formation of data-sharing consortia. *Proceedings of the ACM on Management of Data*, 1(2):1–25, 2023.
- Chen, L., Acun, B., Ardalani, N., Sun, Y., Kang, F., Lyu, H., Kwon, Y., Jia, R., Wu, C.-J., Zaharia, M., et al. Data acquisition: A new frontier in data-centric AI. *arXiv preprint arXiv:2311.13712*, 2023.

- Cook, R. D. Detection of influential observation in linear regression. *Technometrics*, 19(1):15–18, 1977.
- Cover, T. M. *Elements of Information Theory*. John Wiley & Sons, 1999.
- Diamond, S. and Boyd, S. CVXPY: A Python-embedded modeling language for convex optimization. *The Journal of Machine Learning Research*, 17(1):2909–2913, 2016.
- Du, S., Lee, J., Li, H., Wang, L., and Zhai, X. Gradient descent finds global minima of deep neural networks. In *International conference on machine learning*, pp. 1675–1685. PMLR, 2019.
- Dwork, C. Differential privacy. In *International colloquium on automata, languages, and programming*, pp. 1–12. Springer, 2006.
- Dwork, C., McSherry, F., Nissim, K., and Smith, A. Calibrating noise to sensitivity in private data analysis. In *Theory of Cryptography: Third Theory of Cryptography Conference, TCC 2006, New York, NY, USA, March 4-7, 2006. Proceedings 3*, pp. 265–284. Springer, 2006.
- Feldman, V. and Zhang, C. What neural networks memorize and why: Discovering the long tail via influence estimation. *Advances in Neural Information Processing Systems*, 33:2881–2891, 2020.
- Frank, M., Wolfe, P., et al. An algorithm for quadratic programming. *Naval research logistics quarterly*, 3(1-2):95–110, 1956.
- Ghorbani, A. and Zou, J. Data Shapley: Equitable valuation of data for machine learning. In *International Conference on Machine Learning*, pp. 2242–2251. PMLR, 2019.
- Groh, M., Harris, C., Soenksen, L., Lau, F., Han, R., Kim, A., Koochek, A., and Badri, O. Evaluating deep neural networks trained on clinical images in dermatology with the Fitzpatrick 17k dataset. In *Proceedings of the IEEE/CVF Conference on Computer Vision and Pattern Recognition*, pp. 1820–1828, 2021.
- Halabi, S. S., Prevedello, L. M., Kalpathy-Cramer, J., Mamonov, A. B., Bilbily, A., Cicero, M., Pan, I., Pereira, L. A., Sousa, R. T., Abdala, N., et al. The rsna pediatric bone age machine learning challenge. *Radiology*, 290(2):498–503, 2019.
- Hu, E. J., Shen, Y., Wallis, P., Allen-Zhu, Z., Li, Y., Wang, S., Wang, L., and Chen, W. Lora: Low-rank adaptation of large language models. *arXiv preprint arXiv:2106.09685*, 2021.
- Jacot, A., Gabriel, F., and Hongler, C. Neural tangent kernel: Convergence and generalization in neural networks. *Advances in neural information processing systems*, 31, 2018.
- Jaggi, M. Revisiting frank-wolfe: Projection-free sparse convex optimization. In *International conference on machine learning*, pp. 427–435. PMLR, 2013.
- Jia, R., Dao, D., Wang, B., Hubis, F. A., Gurel, N. M., Li, B., Zhang, C., Spanos, C. J., and Song, D. Efficient task-specific data valuation for nearest neighbor algorithms. *arXiv preprint arXiv:1908.08619*, 2019.
- Jiang, K. F., Liang, W., Zou, J., and Kwon, Y. Opendataval: a unified benchmark for data valuation. *arXiv preprint arXiv:2306.10577*, 2023.

- Johnson, A. E., Pollard, T. J., Shen, L., Lehman, L.-w. H., Feng, M., Ghassemi, M., Moody, B., Szolovits, P., Anthony Celi, L., and Mark, R. G. MIMIC-III, a freely accessible critical care database. *Scientific data*, 3(1):1–9, 2016.
- Just, H. A., Kang, F., Wang, J. T., Zeng, Y., Ko, M., Jin, M., and Jia, R. Lava: Data valuation without pre-specified learning algorithms. *arXiv preprint arXiv:2305.00054*, 2023.
- Kallumadi, S. and Grer, F. Drug Review Dataset (Druglib.com). UCI Machine Learning Repository, 2018. DOI: <https://doi.org/10.24432/C55G6J>.
- Karimireddy, S. P., Kale, S., Mohri, M., Reddi, S., Stich, S., and Suresh, A. T. Scaffold: Stochastic controlled averaging for federated learning. In *International conference on machine learning*, pp. 5132–5143. PMLR, 2020.
- Kennedy, J., Subramaniam, P., Galhotra, S., and Castro Fernandez, R. Revisiting online data markets in 2022: A seller and buyer perspective. *ACM SIGMOD Record*, 51(3):30–37, 2022.
- Kornblith, S., Shlens, J., and Le, Q. V. Do better imagenet models transfer better? In *Proceedings of the IEEE/CVF conference on computer vision and pattern recognition*, pp. 2661–2671, 2019.
- Kwon, Y. and Zou, J. Data-oob: Out-of-bag estimate as a simple and efficient data value. *arXiv preprint arXiv:2304.07718*, 2023.
- Lundberg, S. M. and Lee, S.-I. A unified approach to interpreting model predictions. *Advances in neural information processing systems*, 30, 2017.
- McMahan, B., Moore, E., Ramage, D., Hampson, S., and y Arcas, B. A. Communication-efficient learning of deep networks from decentralized data. In *Artificial Intelligence and Statistics*, pp. 1273–1282. PMLR, 2017.
- Paley, R. E. and Zygmund, A. A note on analytic functions in the unit circle. In *Mathematical Proceedings of the Cambridge Philosophical Society*, volume 28, pp. 266–272. Cambridge University Press, 1932.
- Radford, A., Wu, J., Child, R., Luan, D., Amodei, D., Sutskever, I., et al. Language models are unsupervised multitask learners. *OpenAI blog*, 1(8):9, 2019.
- Radford, A., Kim, J. W., Hallacy, C., Ramesh, A., Goh, G., Agarwal, S., Sastry, G., Askell, A., Mishkin, P., Clark, J., et al. Learning transferable visual models from natural language supervision. In *International conference on machine learning*, pp. 8748–8763. PMLR, 2021.
- Sherman, J. and Morrison, W. J. Adjustment of an inverse matrix corresponding to a change in one element of a given matrix. *The Annals of Mathematical Statistics*, 21(1):124–127, 1950.
- Štrumbelj, E. and Kononenko, I. Explaining prediction models and individual predictions with feature contributions. *Knowledge and information systems*, 41:647–665, 2014.
- Travizano, M., Sarraute, C., Dolata, M., French, A. M., and Treiblmaier, H. Wibson: A case study of a decentralized, privacy-preserving data marketplace. *Blockchain and distributed ledger technology use cases: Applications and lessons learned*, pp. 149–170, 2020.
- Tropp, J. A. User-friendly tail bounds for sums of random matrices. *Foundations of computational mathematics*, 12:389–434, 2012.

- Vapnik, V. N. An overview of statistical learning theory. *IEEE transactions on neural networks*, 10 (5):988–999, 1999.
- Wainwright, M. J. *High-Dimensional Statistics: A Non-Asymptotic Viewpoint*, volume 48. Cambridge university press, 2019.
- Wei, J., Bosma, M., Zhao, V. Y., Guu, K., Yu, A. W., Lester, B., Du, N., Dai, A. M., and Le, Q. V. Finetuned language models are zero-shot learners. *arXiv preprint arXiv:2109.01652*, 2021.
- Yoon, J., Arik, S., and Pfister, T. Data valuation using reinforcement learning. In *International Conference on Machine Learning*, pp. 10842–10851. PMLR, 2020.
- Zhao, B., Lyu, B., Fernandez, R. C., and Kolar, M. Addressing budget allocation and revenue allocation in data market environments using an adaptive sampling algorithm. *arXiv preprint arXiv:2306.02543*, 2023.

A Proof of Theorem 1

A.1 Supporting Lemma

Lemma A.1 (Metric entropy, Wainwright (2019)). *Let $\|\cdot\|$ denote the Euclidean norm on \mathbb{R}^d and let \mathbb{B} be the unit balls (i.e., $\mathbb{B} = \{\theta \in \mathbb{R}^d \mid \|\theta\| \leq 1\}$). Then the δ -covering number of \mathbb{B} in the $\|\cdot\|$ -norm obeys the bounds*

$$d \log \left(\frac{1}{\delta} \right) \leq \log N(\delta; \mathbb{B}, \|\cdot\|) \leq d \log \left(1 + \frac{2}{\delta} \right).$$

Lemma A.2 (Fano's inequality, Cover (1999)). *When θ is uniformly distributed over the index set $[M]$, then for any estimator $\hat{\theta}$ such that $\theta \rightarrow Z \rightarrow \hat{\theta}$*

$$\mathbb{P}[\hat{\theta}(Z) \neq \theta] \geq 1 - \frac{I(Z; \theta) + \log 2}{\log M}.$$

Lemma A.3 (Matrix-Chernoff bound, Tropp (2012)). *Consider an independent sequence $\{X_i\}_{i=1}^k$ of random, self-adjoint matrices in M_n satisfying $X_i \geq 0$ and $\lambda_{\max}(X_i) \leq R$ almost surely, for each $i \in \{1, \dots, k\}$. Define*

$$\begin{aligned} \mu_{\min} &:= \lambda_{\min} \left(\sum_{i=1}^k \mathbb{E} X_i \right), \\ \mu_{\max} &:= \lambda_{\max} \left(\sum_{i=1}^k \mathbb{E} X_i \right). \end{aligned}$$

Then,

$$\begin{aligned} \mathbb{P} \left\{ \lambda_{\max} \left(\sum_{i=1}^k X_i \right) \geq (1 + \delta) \mu_{\max} \right\} &< n \left(\frac{e^\delta}{(1 + \delta)^{1 + \delta}} \right)^{\frac{\mu_{\max}}{R}} \quad \text{for } \delta \geq 0; \\ \mathbb{P} \left\{ \lambda_{\min} \left(\sum_{i=1}^k X_i \right) \leq (1 - \delta) \mu_{\min} \right\} &< n \left(\frac{e^{-\delta}}{(1 - \delta)^{1 - \delta}} \right)^{\frac{\mu_{\min}}{R}} \quad \text{for } \delta \in [0, 1]. \end{aligned}$$

Lemma A.4 (Paley–Zygmund inequality, Paley & Zygmund (1932)). *If Z is a random variable with finite variance and $Z \geq 0$ almost surely, then*

$$\mathbb{P}(Z > \theta \mathbb{E}[Z]) \geq (1 - \theta)^2 \frac{\mathbb{E}[Z]^2}{\mathbb{E}[Z^2]}, \quad \forall \theta \in (0, 1).$$

A.2 Proof

Proof. Let $f_\theta(x) = \theta^\top x$ and $\mathcal{E} = N(0, \sigma^2)$. Define the parameter space resulting from the training algorithm:

$$\Theta = \left\{ \hat{\theta}(w) : w \in \Delta([m]) \right\}.$$

When n is sufficiently large, Lemma A.1 implies that there exists $\{\theta_1, \theta_2, \dots, \theta_K\} \subset \Theta$ such that

$$\begin{aligned} \|\theta_i^\top X^{\text{val}}\|_2 &\lesssim \delta \sqrt{n_{\text{val}}}, \quad \forall i \in [K] \\ \|(\theta_i - \theta_j)^\top X^{\text{val}}\|_2 &\asymp \delta \sqrt{n_{\text{val}}}, \quad \forall i < j \in [K]. \end{aligned}$$

Let \mathbb{P}_{θ_i} denote the conditional distribution $\mathcal{D}_{y|x}$ of the target when the underlying model parameter is θ_i , it then follows that

$$\text{KL}(\mathbb{P}_{\theta_i} \|\mathbb{P}_{\theta_i}) \lesssim \frac{n\delta^2}{\sigma^2}.$$

Applying Lemma A.2, we obtain that

$$\inf_{\hat{\theta}} \sup_{\mathcal{D}_{Y|X}, X^{\text{train}}} \mathbb{E} \left[\frac{1}{n_{\text{val}}} \left\| (\hat{\theta}(\hat{w}) - \theta^*)^\top X^{\text{val}} \right\|_2^2 \right] \gtrsim \frac{c_2 \sigma^2 d}{n_{\text{val}}}. \quad (9)$$

Now define $\Sigma = \mathbb{E}_{x \sim \mathcal{D}_X} [xx^\top]$, by Lemma A.3, we have that with probability at least $1 - \exp(-\Omega(n_{\text{val}}/R^2))$,

$$\frac{1}{2}\Sigma \preceq X^{\text{val}}(X^{\text{val}})^\top \preceq 2\Sigma. \quad (10)$$

Notice that

$$\mathbb{E}_{X^{\text{test}}} [\mathcal{L}(\hat{w}) - \mathcal{L}(w^*)] = \left\| (\hat{\theta}(\hat{w}) - \theta^*)^\top \right\|_{\Sigma}^2.$$

Therefore, under the event of Eq. (9), Eq. (10) implies that

$$\begin{aligned} \inf_{\hat{\theta}} \sup_{\mathcal{D}_{Y|X}, X^{\text{train}}} \mathbb{E}_{X^{\text{test}}} [\mathcal{L}(\hat{w}) - \mathcal{L}(w^*)] &\geq \inf_{\hat{\theta}} \sup_{\mathcal{D}_{Y|X}, X^{\text{train}}} \frac{1}{2} \mathbb{E} \left[\frac{1}{n_{\text{val}}} \left\| (\hat{\theta}(\hat{w}) - \theta^*)^\top X^{\text{val}} \right\|_2^2 \right] \\ &\gtrsim \frac{c_2 \sigma^2 d}{n_{\text{val}}} \end{aligned}$$

This establishes the first inequality.

For the second inequality, we have that under the condition $\lambda(\mathbb{E}_{x \sim \mathcal{D}_X} [x^{\otimes 4}]) \leq \kappa \cdot \lambda(\mathbb{E}_{x \sim \mathcal{D}_X} [x^{\otimes 2}]^{\otimes 2})$, the following holds

$$\begin{aligned} \text{Var}_{x \sim \mathcal{D}_X} \left(\left\langle \hat{\theta}(\hat{w}) - \theta^*, x \right\rangle^2 \right) &= \mathbb{E} \left[\left\langle \hat{\theta}(\hat{w}) - \theta^*, x \right\rangle^4 \right] - \mathbb{E} \left[\left\langle \hat{\theta}(\hat{w}) - \theta^*, x \right\rangle^2 \right]^2 \\ &= \mathbb{E} \left[\left\langle (\hat{\theta}(\hat{w}) - \theta^*)^{\otimes 4}, x^{\otimes 4} \right\rangle \right] - \mathbb{E} \left[\left\langle (\hat{\theta}(\hat{w}) - \theta^*)^{\otimes 2}, x^{\otimes 2} \right\rangle^2 \right] \\ &= \left\langle (\hat{\theta}(\hat{w}) - \theta^*)^{\otimes 4}, \mathbb{E} [x^{\otimes 4}] - \mathbb{E} [x^{\otimes 2}]^{\otimes 2} \right\rangle \\ &\leq (\kappa - 1) \cdot \mathbb{E} \left[\left\langle \hat{\theta}(\hat{w}) - \theta^*, x \right\rangle^2 \right]^2. \end{aligned}$$

By Lemma A.4, for any θ and θ^* , we have that with probability at least $0.99 - O\left(\frac{\kappa}{\kappa+m}\right)$,

$$\begin{aligned} \mathcal{L}(\hat{w}) - \mathcal{L}(w^*) &= \frac{1}{m} \left\| (\theta - \theta^*)^\top X^{\text{test}} \right\|_2^2 \\ &= \frac{1}{m} \sum_{i=1}^m \langle \theta - \theta^*, x_i^{\text{test}} \rangle^2 \\ &\geq 0.0001 \cdot \left\| (\hat{\theta}(\hat{w}) - \theta^*)^\top \right\|_{\Sigma}^2 \\ &\gtrsim \frac{c_2 \sigma^2 d}{n_{\text{val}}}. \end{aligned}$$

Combining this and the first inequality by union bound, we establish the second inequality. \square

B Convergence rate of Frank-Wolfe

Consider the following problem:

$$\min_{x \in \mathcal{D}} f(x).$$

Define the duality gap

$$g(x) = \sup_{s \in \mathcal{D}} \langle x - s, \nabla f(x) \rangle.$$

Define the curvature constant

$$C_f = \sup_{s, x \in \mathcal{D}, \gamma \in (0, 1), y = (1-\gamma)x + \gamma s} \frac{2}{\gamma^2} (f(y) - f(x) - \langle y - x, \nabla f(x) \rangle).$$

Frank-Wolfe:

- for $k = 1, 2, \dots$,
 - $\langle s^{(k)}, \nabla f(x^{(k)}) \rangle \leq \min_{t \in \mathcal{D}} \langle t, \nabla f(x^{(k)}) \rangle + \frac{1}{2} \delta \gamma^{(k)} C_f$
 - $x^{(k+1)} = \gamma^{(k)} \cdot s^{(k)} + (1 - \gamma^{(k)}) \cdot x^{(k)}$

Lemma B.1 (Lemma 5, Jaggi (2013)). *For any $\gamma \in (0, 1)$,*

$$f(x^{(k+1)}) \leq f(x^{(k)}) - \gamma^{(k)} g(x^{(k)}) + \frac{(\gamma^{(k)})^2}{2} C_f (1 + \delta).$$

Theorem B.2. *In the Frank-Wolfe algorithm, if $\gamma^{(k)}$ is set to $\frac{1}{k+1}$ for every k , then*

$$f(x^{(k)}) \leq f(x^*) + \frac{C \log k}{k}$$

where $C = C_f(1 + \delta)$.

Proof. Define $h(x) = f(x) - f(x^*)$. Using Lemma B.1,

$$\begin{aligned} h(x^{(k)}) &\leq h(x^{(k-1)}) - \gamma^{(k-1)} g(x^{(k-1)}) + \frac{(\gamma^{(k-1)})^2}{2} C_f (1 + \delta) \\ &\leq h(x^{(k-1)}) - \gamma^{(k-1)} h(x^{(k-1)}) + \gamma^{(k-1)2} C \\ &= (1 - \gamma^{(k-1)}) h(x^{(k-1)}) + \gamma^{(k-1)2} C \\ &= \frac{k-1}{k} h(x^{(k-1)}) + \frac{C}{k^2} \\ &\leq \frac{k-2}{k} h(x^{(k-2)}) + \frac{C}{k(k-1)} + \frac{C}{k^2} \\ &\leq \dots \\ &\leq \sum_{i=1}^k \frac{C}{k \cdot i} \\ &\leq \frac{C \log k}{k}. \end{aligned}$$

□

Using a step-size $\gamma^{(k)} = \frac{1}{k+1}$ produces final iterate with uniform weights i.e.

$$x^{(k)} = \frac{1}{k} \sum_{i=0}^{k-1} s^{(i)}.$$

Thus, in our case we will have $w = \sum_{i=0}^{k-1} e_{i_k} \in \{0, 1\}^k$. Hence, we showed a $O(1/k)$ approximation to the otherwise intractable combinatorial problem. With additional assumptions on the structure of the loss function, one can even show improved quadratic or even exponential approximations (Bach et al., 2012).

C Additional Experimental Details

For each buyer test point, we optimize each selection algorithm over the 1,000 seller data points and select the highest value data based on the validation set of 100 data points (our method and Data OOB do not use the validation set). For each test point, we train a linear regression model on the selected seller points and report test mean squared error (MSE) on the buyer’s data and average test error over 100 buyers.

We benchmarked all results on an Intel Xeon E5-2620 CPU with 40 cores and a Nvidia GTX 1080 Ti GPU. For baseline implementation of data valuation methods, we use the OpenDataVal package Jiang et al. (2023) version 1.2.1. We use the default hyperparameter settings for all methods with the exception of Data Shapley (changed 100 Monte-Carlo epochs with 10 models per iteration), Influence Subsample (from 1000 to 500 models), and Data OOB (from 1000 to 500 models) to reduce computational runtime.

For the Gaussian dataset, we generate a regression dataset according to the following Python code:

```

1 import numpy as np
2
3 def get_gaussian_data(num_samples=100, dim=10, noise=0.1, costs=None):
4     X = np.random.normal(size=(num_samples, dim))
5     X /= np.linalg.norm(X, axis=1, keepdims=True)
6     if costs is not None:
7         X *= costs
8     coef = np.random.exponential(scale=1, size=dim)
9     coef *= np.sign(np.random.uniform(low=-1, high=1, size=dim))
10    y = X @ coef + noise * np.random.randn(num_samples)
11    return dict(X=X, y=y, coef=coef, noise=noise, dim=dim, costs=costs)

```

For the DrugLib dataset, we format each review using the following prompt template to feed GPT-2:

```

Benefits: $BENEFITS_REVIEW
Side effects: $SIDE_EFFECTS_REVIEW
Comments: $COMMENTS_REVIEW

```

where \$BENEFITS_REVIEW is the corresponding portion of the drug review.

We will release all experimentation code upon acceptance.

D Additional Experiments

D.1 Number of Seller Data

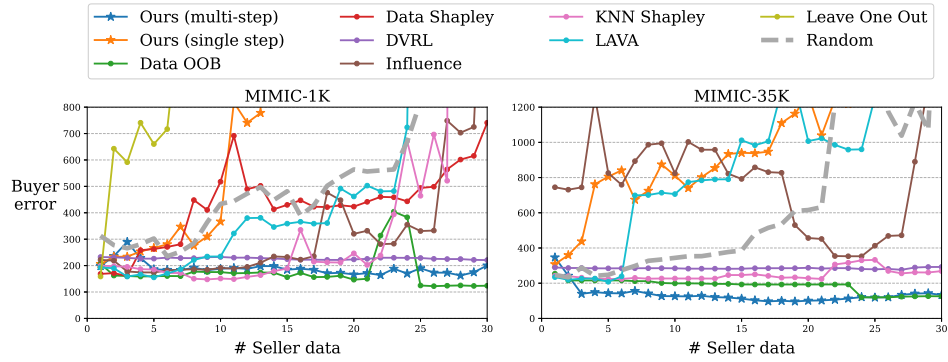


Figure 9: Comparison of buyer prediction error across data selection methods on the MIMIC dataset with 1,000 seller data points (left subplot) and 35,000 seller data points (right).

D.2 Budget Results

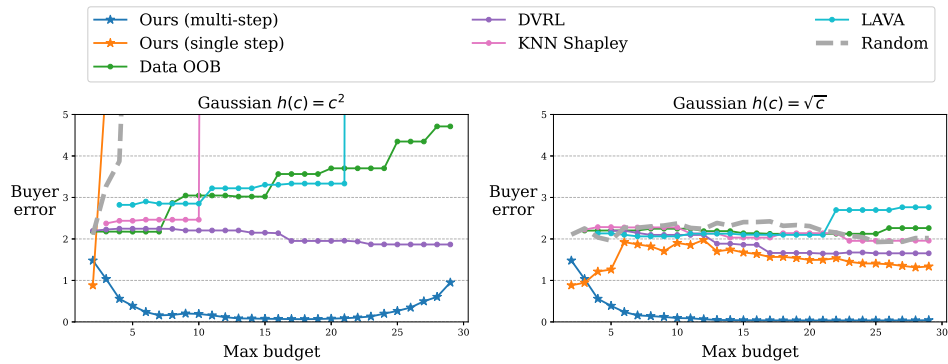


Figure 10: Comparing data selection algorithms on Gaussian-10K dataset with different cost functions.

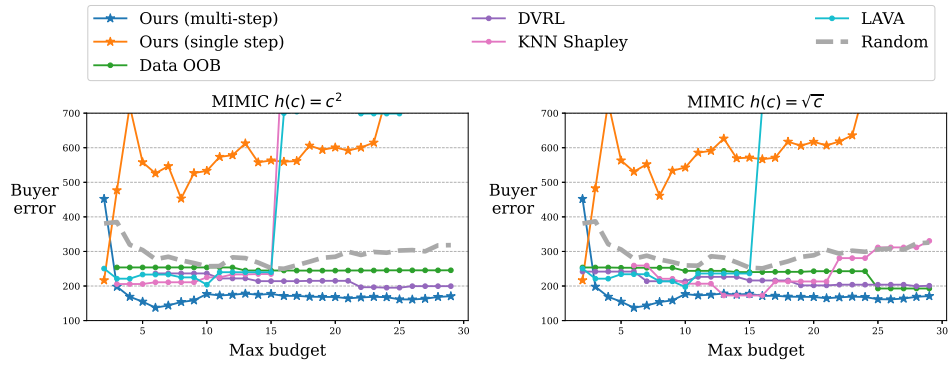


Figure 11: Comparing data selection algorithms on MIMIC-35K dataset with different cost functions.

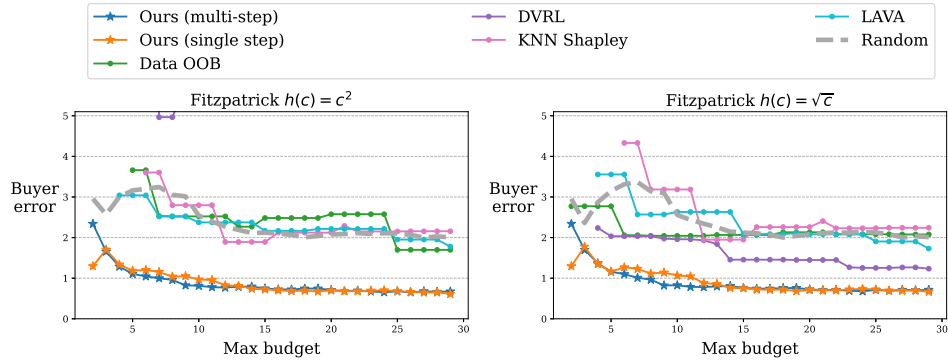


Figure 12: Comparing data selection algorithms on Fitzpatrick-15K dataset with different cost functions.

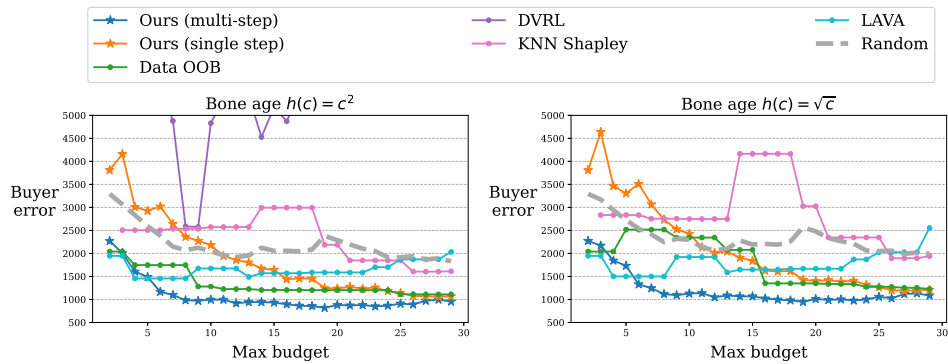


Figure 13: Comparing data selection algorithms on Bone age-12K dataset with different cost functions.

	Gaussian		MIMIC		Bone age		Fitzpatrick		Druglib	
COST FUNCTION	\sqrt{c}	c^2	\sqrt{c}	c^2	\sqrt{c}	c^2	\sqrt{c}	c^2	\sqrt{c}	c^2
Random baseline	2.26	77.7	288.3	284.6	2253.8	2065.0	2.14	2.11	16.5	18.4
DVRL	1.67	2.1	213.9	214.5	24003.1	5588.3	1.46	8.90	22.5	20.7
LAVA	2.13	3.3	482.1	474.6	1666.9	1586.7	2.09	2.21	35.7	34.8
KNN Shapley	2.13	69.0	217.1	956.0	2753.9	2505.8	1.85	2.15	13.6	13.0
Data OOB	2.19	3.3	242.8	245.4	1695.3	1205.2	2.08	2.52	10.8	10.8
Ours (single step)	1.54	251.5	598.4	585.1	1734.3	1550.0	0.75	0.71	9.4	10.1
Ours (multi-step)	0.04	0.2	168.9	168.7	1076.3	942.1	0.76	0.75	12.6	11.4

Table 2: Comparing data selection methods for two different cost functions, $h = \sqrt{c}$ and $h = c^2$. For each budget constraint, we select seller points until the budget is exceeded and calculate test prediction error on the buyer data. We average over 100 buyers and report the median test error across budgets from 1 to 30.

D.3 Runtime Comparison

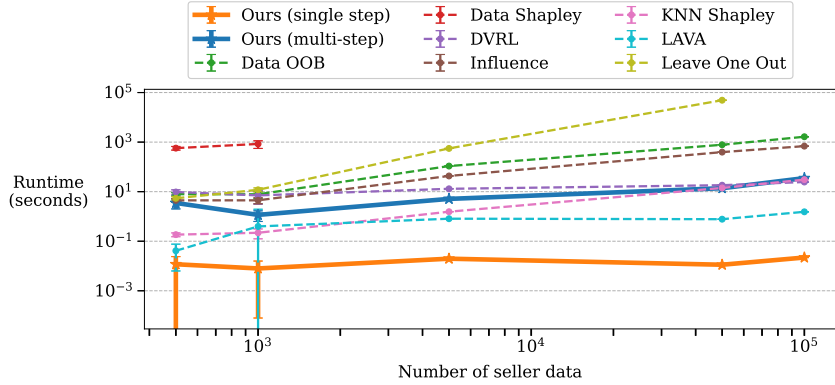


Figure 14: Runtime comparison with increasing number of data points.

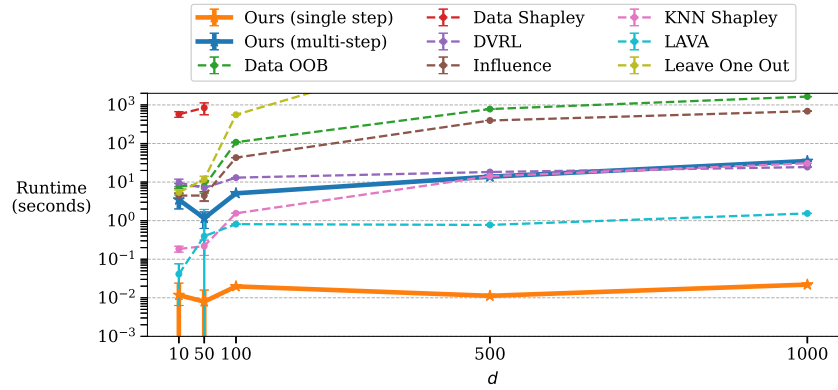


Figure 15: Runtime comparison with increasing dimensionality.

D.4 Iterative versus Convex optimization

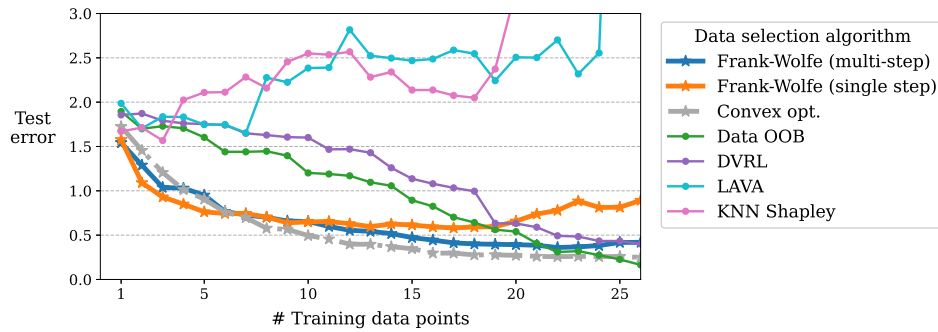


Figure 16: Comparing prediction error of Frank-Wolfe optimization with Convex optimization on 1000 data points sampled from 30-dimensional Gaussian. Averaged over 100 test points.

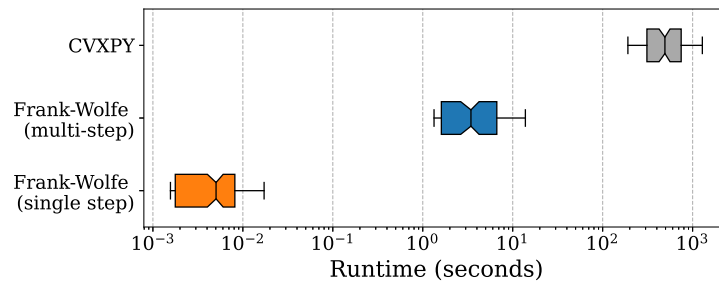


Figure 17: Comparing runtime of Frank-Wolfe optimization with Convex optimization on 1000 data points sampled from 30-dimensional Gaussian. Averaged over 100 test points.

D.5 Regularization

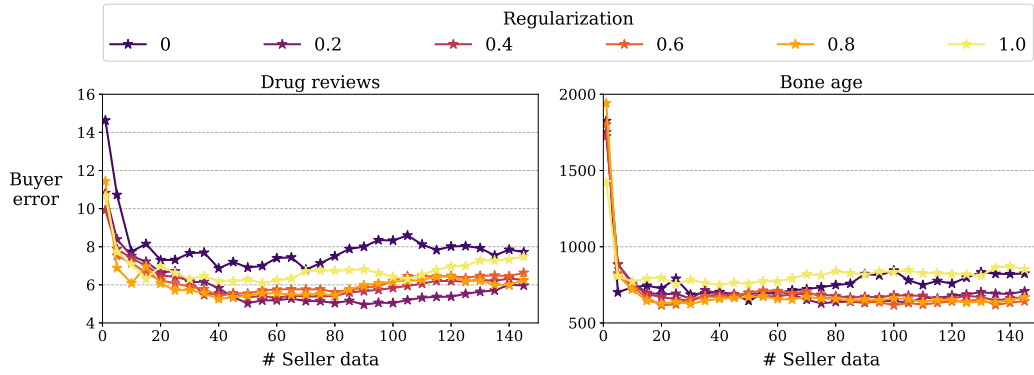


Figure 18: Varying the strength of regularization on DrugLib and Bone Age datasets.

D.6 Number of Test Data

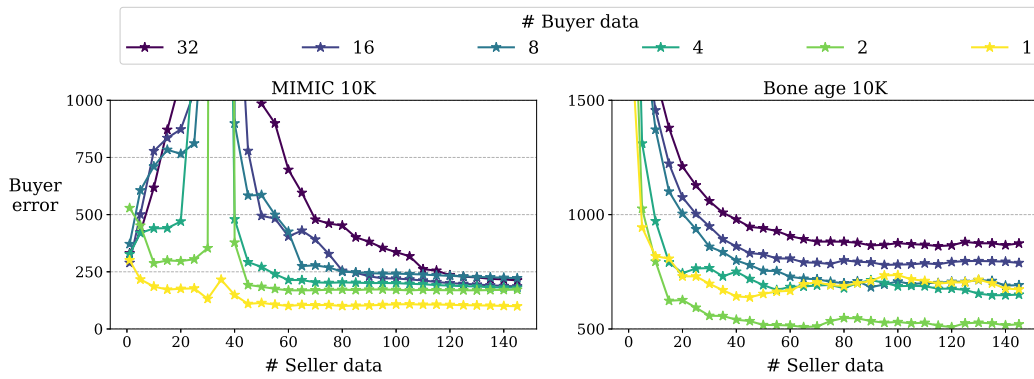


Figure 19: Varying the number of buyer test points on MIMIC and Bone Age datasets.

D.7 Number of Iteration Steps

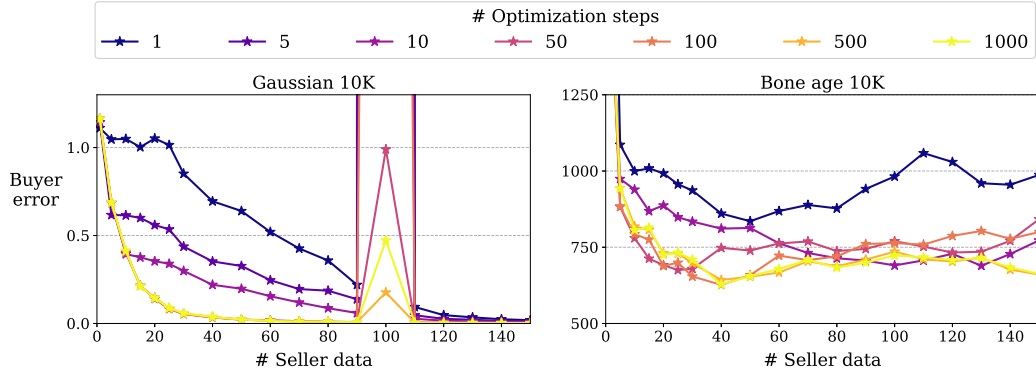


Figure 20: Varying the number of optimization steps on Gaussian and Bone Age datasets.